The activity of Fe–Pd alloys for the water–gas shift reaction

S. Zhao* and R. J. Gorte

Department of Chemical & Biomolecular Engineering, University of Pennsylvania, Philadelphia, PA 19104, USA

Received 23 September 2003; accepted 4 November 2003

The role of Fe promoters has been investigated on Pd/ceria, Pt/ceria and Rh/ceria catalysts for the water–gas shift (WGS) reaction in 25 torr of CO and H_2O under differential reaction conditions. While no enhancement was observed with Pt and Rh, the activity of Pd/ceria increased by as much as an order of magnitude upon the addition of an optimal amount of Fe. Similarly, the addition of 1 wt% Pd to an Fe_2O_3 catalyst increased the WGS rate at 453 K by a factor of 10 over that measured on Fe_2O_3 alone, while the addition of Pt or Rh to Fe_2O_3 had no effect on rates. The amount of Fe that was necessary to optimize the rates increased with Pd loading but was independent of the order in which Fe and Pd were added to the ceria. Increased WGS activity was also observed upon the addition of Fe to Pd supported on $Ce_{0.5}Zr_{0.5}O_2$. XRD measurements, performed after running the catalyst under WGS conditions, show the formation of a Fe–Pd alloy, even though similar measurements on an Fe/ceria catalyst showed that Fe_3O_4 was the stable phase for Fe in the absence of Pd. Possible implications of these results on the development of new WGS catalysts are discussed.

KEY WORDS: water–gas shift; Pd; Pt; Rh; Fe; FePd alloys; ceria.

1. Introduction

There is a need for better water–gas shift (WGS) catalysts for the development of efficient fuel processors for fuel-cell applications [1,2]. Getting higher WGS activities is crucial because it would allow the reaction to be carried out at lower temperatures where the equilibrium concentration of CO, a serious poison for low-temperature fuel cells, is decreased. Materials that are typically used for the WGS reaction in large-scale operations, such as Cu/ZnO, are not applicable for many fuel-cell applications due to the fact that they are sensitive to start-up/shutdown cycles and may be pyrophoric [1,2]. Ceria-supported, precious-metal catalysts are one class of materials that have been identified as exhibiting very interesting properties for the WGS reaction with fuel cells [1–6]. The properties of ceria-supported precious metals are well known because of their application to automotive, emissions-control catalysis; however, the application of these materials to low-temperature WGS will require optimization in a very different manner.

While ceria-supported precious metals can exhibit higher rates than that obtained on commercially available Cu/ZnO catalysts under some conditions of interest for fuel-cell applications [1,4], even higher activities would be desirable to offset the cost of the precious metals. In recent work from our laboratory [7], the effect of a large number of promoters was investigated on Pd/ceria catalysts. The majority of these "promoters" (Tb, Gd, Y, Sn, Sm, Pr, Eu, Bi, and Cr) had minimal effect on the catalytic activity. A few others (V, Pb, and Mo) decreased WGS rates over Pd/ceria. However, rates on the Fe-promoted samples were found to be as much as eight times higher than that on unpromoted Pd/ceria at 473 K. Furthermore, there was an optimum Fe content that gave rise to the highest rates.

In the present study, we set out to investigate the reason for the enhancement in the WGS activity found on Pd/ceria. What we will show is that the enhanced activity associated with adding Fe_2O_3 to Pd/ceria is due to the formation of an Fe–Pd alloy. The addition of Fe_2O_3 did not enhance the rates on Pt/ceria or Rh/ceria, suggesting that there may be something unique about the Fe–Pd system. Interestingly, the stable form of Fe under WGS conditions in the absence of Pd is Fe_3O_4, suggesting that formation of the alloy provides a driving force for the reduction of Fe.

2. Experimental

The ceria used for all the measurements in this study was synthesized by decomposition of $Ce(NO_3)_3 \cdot 6H_2O$ (Alfa Aesar, 99.5%) in air at 873 K. A ceria-zirconia mixed oxide ($Ce_{0.5}Zr_{0.5}O_2$) was also prepared by mixing aqueous solutions of $ZrO(NO_3)_2 \cdot xH_2O$ (Aldrich) and $Ce(NO_3)_3 \cdot 6H_2O$, then drying the mixed solution at 383 K overnight, and finally calcining the dried powder in air at 873 K for 4 h. The Fe_2O_3 sample that was used as a support was prepared by decomposing $Fe(NO_3)_3 \cdot 9H_2O$ (Aldrich, 99.99+ %) in air at 873 K. For most experiments, Fe was added to the ceria or ceria-zirconia supports by aqueous impregnation with

* To whom correspondence should be addressed.

1011-372X/04/0100–0075/0 © 2004 Plenum Publishing Corporation

Table 1
BET surface areas of supports used in this study, after outgassing at 623 K

Support	BET surface area (m^2/g)
CeO_2	61
$Ce_{0.5}Zr_{0.5}O_2$	84
Fe-ceria, 0.7 wt% Fe_2O_3	64
Fe-ceria, 1.4 wt% Fe_2O_3	64
Fe-ceria, 2.2 wt% Fe_2O_3	60
Fe-ceria, 2.9 wt% Fe_2O_3	54
Fe-ceria, 5.7 wt% Fe_2O_3	43
Fe-ceria, 11.4 wt% Fe_2O_3	41
Fe_2O_3	12

$Fe(NO_3)_3 \cdot 9H_2O$. After impregnation with the $Fe(NO_3)_3 \cdot 9H_2O$, the samples were again dried at 383 K overnight and calcined in air at 873 K for 4 h. The BET surface areas for the supports used in this study are shown in table 1, with the Fe loadings calculated as weight percent Fe_2O_3.

The precious metals were also added to the oxide supports by wet impregnation using aqueous solutions of $Pd(NH_3)_4(NO_3)_2$ (Aldrich, 99.99%), $Pt(NH_3)_4(NO_3)_2$ (Alfa Aesar, 99.99%) or $Rh(NO_3)_3$ (Alfa Aesar, 99.9%). Following impregnation of the precious metal salts, the catalysts were dried at 383 K and calcined at 873 K. To determine whether the order in which Pd and Fe were added to ceria was important, we prepared a sample with 1 wt% Pd and 2.2 wt% Fe_2O_3 in which $Pd(NH_3)_4(NO_3)_2$ was added first, dried overnight, and finally calcined in air at 873 K for 4 h before adding $Fe(NO_3)_3 \cdot 9H_2O$. Still other catalysts were prepared by coimpregnation of Fe and Pd onto the ceria support, again using aqueous solutions of $Fe(NO_3)_3$ and $Pd(NH_3)_4(NO_3)_2$ and similar drying and calcination procedures.

The WGS reaction rates were measured in a quarter-inch Pyrex tubular reactor using 0.10 g of catalyst. Water was introduced by saturation of a He carrier gas flowing through a bubbler with deionized water. While the reactor pressure was always atmospheric, the partial pressures of CO, H_2O and He were controlled by adjusting the relative flow rates of each component. All the reaction measurements in this study were collected with partial pressures for CO and H_2O of 25 torr. All the reaction rates were measured under differential conditions, with the conversions of CO and H_2O kept below 10%. To avoid potential transients associated with catalyst oxidation and reduction, we always allowed the reaction to run for at least 30 min before analyzing the products. To ensure that the results were reproducible, the rates at each point were measured at least three times. The concentration of the effluent from the reactor was determined using an on-line gas chromatograph, SRI8610C, equipped with a Hayesep Q column and a TCD detector.

Phase identification in the samples was performed via X-ray diffraction with a Rigaku X-ray diffractometer, using Ni-filtered, Cu Kα radiation ($\lambda = 1.54184$ Å). The diffraction measurements were performed in the range of $2\theta = 30$–50° with a scanning speed of 2° 2θ/min.

3. Results and discussion

The first evidence that the addition of Fe to the ceria support must do more than simply modify the properties of the ceria support came from WGS rate measurements with various Fe:Pd ratios, with representative data for the Fe-impregnated ceria catalysts reported in figure 1 and table 2. Figure 1 shows Arrhenius plots for the WGS reaction, in 25 torr of both CO and H_2O, with results for catalysts with 1 wt% Pd shown in figure 1(a) and results for catalysts with 2 wt% Pd shown in figure 1(b). In order to maintain differential conversions, it was necessary to use a higher temperature range for the less active catalysts, so that the most active catalysts are those for which the data are on the upper right of the plots. In agreement with the earlier study of Pd on Fe-doped ceria [7], the activities of the Pd catalysts prepared with Fe-doped ceria were higher than that with undoped ceria; and there is an optimal Fe content for maximizing the rates. However, the optimum Fe content was different for the two Pd loadings. For 1 wt% Pd, the maximum rates occur with 2.2 wt% Fe_2O_3; with 2 wt% Pd, the maximum rates occur at 4.3 wt% Fe_2O_3. In both these catalysts, the Fe:Pd molar ratio is the same, approximately 3:1.

Table 2 summarizes the data in figure 1 by giving the rates and activation energies at 453 K for each of the catalysts. As might be expected, rates with 2 wt% Pd on pure ceria were approximately twice that of the rates on the 1 wt% catalysts. Pd/Fe_2O_3 showed rates that were comparable to Pd/ceria, but both of these catalysts were much less active than the catalysts containing all three components. In agreement with an earlier study [7], the activation energy of the Fe-containing catalysts was somewhat higher than that found on Pd/ceria. Finally, it should be noted that the activity of 2.2 wt% Fe_2O_3 on ceria, extrapolated to 453 K, is expected to be only 0.0012×10^{18} molecules/s/g, much lower than any of the Pd-containing catalysts.

The fact that there is a specific Fe–Pd stoichiometry associated with maximum WGS activity suggests that Fe–Pd compounds could be responsible for the increased activity. In this case, it would be expected that the order in which Pd and Fe are added to the catalyst should not matter. To explore this possibility, we prepared ceria-supported catalysts with 2.2 wt% Fe_2O_3 and 1 wt% Pd by coimpregnation of the Pd and Fe precursor salts and by impregnating Pd before Fe. The rate data for these three samples are listed in table 3 and

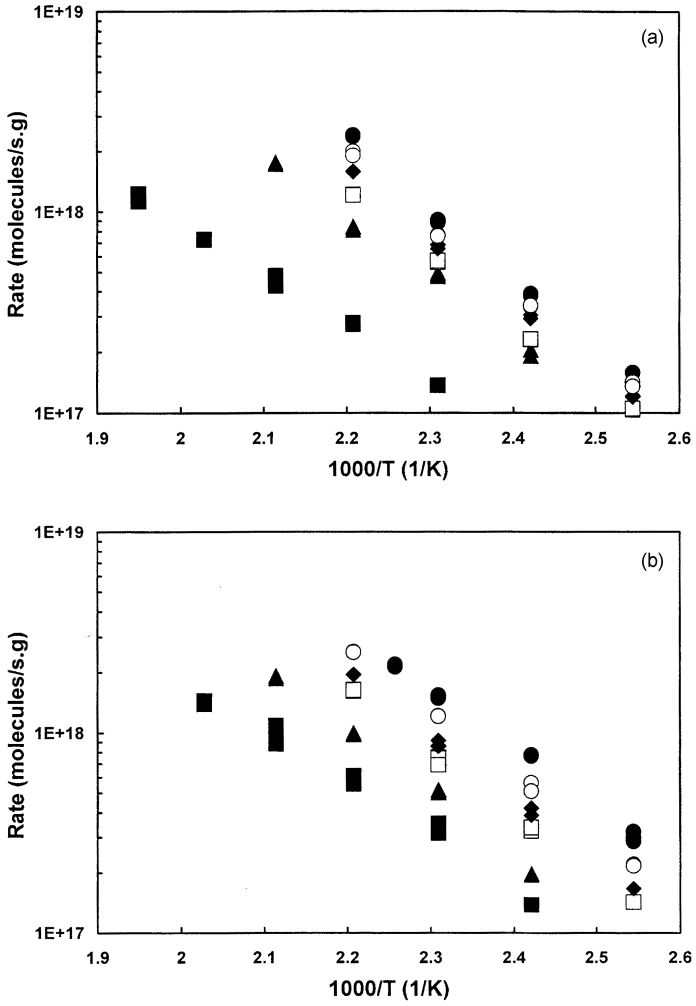

Figure 1. (a) Differential rates for the WGS reaction on 1% Pd/ceria (■), 1% Pd/Fe/ceria (0.7 wt% Fe_2O_3) (▲), 1% Pd/Fe/ceria (1.4 wt% Fe_2O_3) (◆), 1% Pd/Fe/ceria (2.2 wt% Fe_2O_3) (●), 1% Pd/Fe/ceria (2.9 wt% Fe_2O_3) (○), 1% Pd/Fe/ceria (5.7 wt% Fe_2O_3) (□). (b) Differential rates for the WGS reaction on 2% Pd/ceria (■), 2% Pd/Fe/ceria (0.7 wt% Fe_2O_3) (▲), 2% Pd/Fe/ceria (2.2 wt% Fe_2O_3) (○), 2% Pd/Fe/ceria (4.3 wt% Fe_2O_3) (●), 2% Pd/Fe/ceria (5.7 wt% Fe_2O_3) (◆), 2% Pd/Fe/ceria (11.4 wt% Fe_2O_3) (□).

Table 2
Differential rates and activation energies for the water–gas shift reaction on Fe promoted, Pd/Ceria catalysts

	Catalyst	Rate at 453 K ($\times 10^{18}$ molecules/s/g_{cat})	Activation energy (kJ/mol)
1 wt% Pd	Pd/ceria	0.27	49
	Pd/Fe-ceria (0.7 wt% Fe_2O_3)	0.84	52
	Pd/Fe-ceria (1.4 wt% Fe_2O_3)	1.58	60
	Pd/Fe-ceria (2.2 wt% Fe_2O_3)	2.42	67
	Pd/Fe-ceria (2.9 wt% Fe_2O_3)	1.91	61
	Pd/Fe-ceria (5.7 wt% Fe_2O_3)	1.21	57
	Pd/Fe_2O_3	0.47	55
2 wt% Pd	Pd/ceria	0.61	43
	Pd/Fe-ceria (0.7 wt% Fe_2O_3)	0.98	61
	Pd/Fe-ceria (2.2 wt% Fe_2O_3)	2.52	60
	Pd/Fe-ceria (4.3 wt% Fe_2O_3)	3.15	61
	Pd/Fe-ceria (5.7 wt% Fe_2O_3)	1.95	60
	Pd/Fe-ceria (11.4 wt% Fe_2O_3)	1.63	62
	Pd/Fe_2O_3	0.29	47
Fe/ceria (Fe_2O_3: 2.2 wt%)		0.0012[a]	80

[a] The reaction rate was extrapolated from higher temperature data.

Table 3
The effect of preparation conditions for Pd/Fe-ceria

Catalyst	Rate at 453 K ($\times 10^{18}$ molecules/s/g_{cat})	Activation energy (kJ/mol)
1 wt% Pd/ceria	0.27	49
1 wt% Pd/Fe-ceria[a] (2.2 wt% Fe_2O_3)	2.42	67
Fe/1 wt% Pd-ceria[b] (2.2 wt% Fe_2O_3)	2.21	52
1 wt% Pd/Fe-ceria[c] (2.2 wt% Fe_2O_3)	2.89	59

[a]Fe_2O_3 was loaded onto ceria first, then Pd was loaded.
[b]Pd was loaded onto ceria first, then Fe_2O_3 was loaded.
[c]Pd and Fe_2O_3 were loaded onto ceria by coimpregnation.

Table 4
Differential rates and activation energies for the water–gas shift reaction on Fe-modified Pt/ceria and Rh/ceria catalysts

	Catalyst	Rate at 453 K ($\times 10^{18}$ molecules/s/g_{cat})	Activation energy (kJ/mol)
1 wt% Pd	Pt/ceria	0.24	61
	Pt/Fe-ceria (0.7 wt% Fe_2O_3)	0.24	69
	Pt/Fe-ceria (1.4 wt% Fe_2O_3)	0.28	73
	Pt/Fe-ceria (2.2 wt% Fe_2O_3)	0.29	73
	Pt/Fe-ceria (2.9 wt% Fe_2O_3)	0.25	66
	Pt/Fe-ceria (5.7 wt% Fe_2O_3)	0.27	71
1 wt% Rh	Rh/ceria	0.23	55
	Rh/Fe-ceria (2.2 wt% Fe_2O_3)	0.23	57
	Rh/Fe-ceria (2.9 wt% Fe_2O_3)	0.25	58
	Rh/Fe-ceria (5.7 wt% Fe_2O_3)	0.23	58

demonstrate that there is no significant difference between the three samples.

To determine whether Fe could also promote Pt and Rh catalysts, we investigated 1 wt% Pt and Rh catalysts on some of the same supports listed in table 1, with the rates reported in table 4. At 453 K, the rates on Pt/ceria and Rh/ceria are essentially identical to that which we observed on undoped Pd/ceria, although the activation energies on the Pt and Rh catalysts were slightly higher. What is more striking about the rates in table 4 is the fact that the addition of Fe had no measurable effect on the rates with Pt- and Rh-based catalysts. Table 5, which gives the WGS rates for each of the precious metals when supported on pure Fe_2O_3, also demonstrates that enhanced rates only occur with Pd. The Fe_2O_3-supported Pt and Rh catalysts showed rates that were indistinguishable from that over the Fe_2O_3 catalyst itself.

Table 5
Differential rates and activation energies for the water–gas shift reaction for Pd, Pt, and Rh supported on Fe_2O_3

Catalyst[a]	Rate at 453 K ($\times 10^{18}$ molecules/s/g_{cat})	Activation energy (kJ/mol)
Fe_2O_3	0.04[b]	58
Pd/Fe_2O_3	0.84	55
Pt/Fe_2O_3	0.09	70
Rh/Fe_2O_3	0.06	69

[a]Pd, Pt, and Rh loading were 1 wt%.
[b]Rate was extrapolated from higher temperature data.

Since ceria-zirconia mixed oxides are usually found to be more active and stable than pure ceria, we measured reaction rates for 1 wt% Pd, Pt, and Rh on the $Ce_{0.5}Zr_{0.5}O_2$ support, both with and without the addition of Fe, with the results shown in table 6. First, the rates for each of the precious metals on the $Ce_{0.5}Zr_{0.5}O_2$ support were very similar to the rates on pure ceria. Again, the addition of 2.9 wt% Fe_2O_3 led to a significant enhancement with the Pd catalyst, but there was essentially no change in rates upon the addition of Fe to the Pt and Rh catalysts.

To identify the phases responsible for the high activity in the Pd/Fe-ceria catalyst, we prepared the following catalysts: 6 wt% Pd on ceria; 13 wt% Fe_2O_3 on ceria and 6 wt% Pd, 13 wt% Fe_2O_3 on ceria. Each sample was then exposed to the same WGS reaction conditions at 473 K for 2 h, then cooled in He to room temperature. Because initial experiments showed that the samples were reoxidized when exposed to air at room temperature, we first passed 1-butene over the catalysts for 30 min at room temperature, before taking the samples out of the reactor, since the carbon-covered catalysts are not as susceptible to reoxidation. Figure 2 shows a

Table 6
Differential rates and activation energies for the water–gas shift reaction on $Ce_{0.5}Zr_{0.5}O_2$-supported Pt, Pd, and Rh catalysts

Catalyst[a]	Rate at 453 K ($\times 10^{18}$ molecules/s/g_{cat})	Activation energy (kJ/mol)
$Fd/Ce_{0.5}Zr_{0.5}O_2$	0.34	49
$Pd/Fe\text{-}Ce_{0.5}Zr_{0.5}O_2$ (Fe_2O_3: 2.9 wt%)	1.97	58
$Pt/Ce_{0.5}Zr_{0.5}O_2$	0.30	50
$Pt/Fe\text{-}Ce_{0.5}Zr_{0.5}O_2$ (Fe_2O_3: 2.9 wt%)	0.26	47
$Rh/Ce_{0.5}Zr_{0.5}O_2$	0.21	47
$Rh/Fe\text{-}Ce_{0.5}Zr_{0.5}O_2$ (Fe_2O_3: 2.9 wt%)	0.19	55

[a]Pd, Pt and Rh loading were 1 wt%.

comparison of XRD patterns on the three catalysts in the range of 30 to 50° 2θ. The metallic Pd peak at 40.12° 2θ was clearly observed for 6 wt% Pd/ceria. On the basis of the Scherrer analysis of the peak width at half height, we estimate the average Pd particle size to be approximately 7 nm, in reasonable agreement with a previous report showing the Pd particle size after the WGS reaction [8]. On the Fe_2O_3/ceria sample, the peak at 36.85° 2θ shows that Fe remains in an oxidized form, but as Fe_3O_4. The 6 wt% Pd, 13 wt% Fe_2O_3 sample still shows the peak that we associate with Fe_3O_4, but now the peak associated with Pd has shifted upward to near 41.22° 2θ, which would be associated with the (111) plane of the alloy, Fe–Pd. The diffraction lines remain broad due to the small metal particle sizes, but there may also be particles with a range of compositions. Finally, it is noteworthy that others have also reported that Fe–Pd alloys can form when Pd is deposited onto supports containing Fe_2O_3 [9].

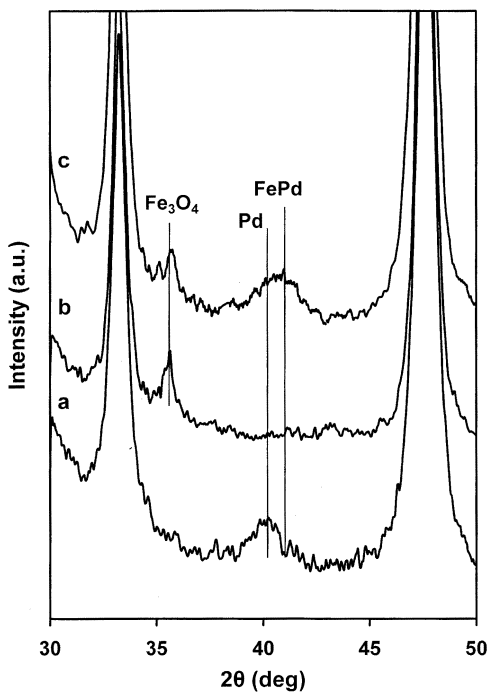

Figure 2. XRD data for (a) 6% Pd/ceria, (b) Fe/ceria (13 wt% Fe_2O_3) and (c) 6% Pd/Fe-ceria (13 wt% Fe_2O_3). Samples were pretreated in the WGS condition at 473 K for 2 h. For Fe/ceria (13 wt% Fe_2O_3) and 6% Pd/Fe-ceria (13 wt% Fe_2O_3), after treatment under WGS conditions, cooling to room temperature, and then exposure to 1-butene to prevent sample reoxidation.

Our finding that Fe exists as Fe_3O_4 under WGS conditions agrees with previous work on Fe-based catalysts and with thermodynamic calculations of the expected phase for Fe under these conditions [10]. For the Fe–Pd alloy to form under the same conditions implies that formation of the alloy must provide an energetic driving force for reduction of Fe. The phase diagram for the Pd–Fe system shows two alloy phases, a FePd phase and a $FePd_3$ phase [11]. Since the maximum rates seem to occur in catalysts for which the Fe:Pd ratio is ~3, a large excess over the 1:1 ratio in FePd, and since Fe_3O_4 is observed together with the FePd phase under WGS conditions, there may be an equilibrium between Fe_3O_4 and FePd. This may explain why Pt and Rh catalysts are not affected in the same way as Pd catalysts. If alloys had formed with Pt and Rh, one should expect that the reaction rates on those catalysts would have been affected, either positively or negatively. While alloys of these metals with Fe do exist, there is evidence that they do not form as readily as FePd [12]. Finally, it is interesting to observe that Pd–Zn alloys also exhibit unique properties for steam reforming of methanol [13].

A thermodynamic driving force for reducing Fe_3O_4 could explain the enhanced WGS activity that is observed for these catalysts. In previous work from our laboratory [5], it has been proposed that the WGS reaction over ceria-supported precious metals proceeds through a redox mechanism, as shown below:

$$CO + \sigma \rightarrow CO_{ad} \quad (1)$$

$$H_2O + Ce_2O_3 \rightarrow 2CeO_2 + H_2 \quad (2)$$

$$CO_{ad} + 2CeO_2 \rightarrow CO_2 + Ce_2O_3 + \sigma \quad (3)$$

According to this picture, CO adsorbs on the precious-metal sites (σ) and the adsorbed CO is then oxidized with oxygen from the ceria; the reduced ceria is then reoxidized by H_2O. If Fe, by its intimate contact with Pd, can enhance either the oxidation by water or

reduction by CO, one should expect increased reaction rates for the alloy catalyst.

Independent of what mechanism is responsible for the rate enhancement upon formation of the Fe–Pd alloy, the results are intriguing in that they suggest that this and other alloys could prove to be interesting WGS catalysts. In addition to increasing reaction rates, alloy catalysts could exhibit increased stabilities and possibly allow decreased loadings of the precious metal. Certainly, the observation that Fe–Pd alloys show significantly higher reaction rates suggests that the combination of precious and base metals is an avenue worth exploring.

4. Conclusion

We have demonstrated that the enhanced WGS activity observed upon the addition of Fe to Pd/ceria catalysts is probably due to the formation of an Fe–Pd alloy. Under WGS conditions, Fe would normally exist as Fe_3O_4, suggesting that formation of the alloy could provide a thermodynamic driving force for Fe reduction. Enhanced WGS activity was not observed upon the addition of Fe to either Pt or Rh catalysts, providing further evidence that specific interactions between Fe and Pd must be responsible for the higher rates observed in materials containing both elements.

Acknowledgment

This work was supported by the DOE, Basic Energy Sciences, Grant #DE-FG03-85-13350.

References

[1] A.F. Ghenciu, Curr. Opin. Solid State Mater. Sci. 6 (2002) 389.
[2] J.R. Ladebeck and J.P. Wagner, in *Handbook of Fuel Cell Technology—Fundamentals, Technology, and Applications,* Chapter 17, W. Vielstich *et al*. (eds) (Wiley, 2003)
[3] Q. Fu, H. Saltsburg and M. Flytzani-Stephanopoulos, Science 301 (2003) 935.
[4] S.L. Swartz, M.M. Seabaugh, C.T. Holt and W.J. Dawson, Fuel Cell Bull. 4 (2001) 7.
[5] T. Bunluesin, R.J. Gorte and G.W. Graham, Appl. Catal. B 15 (1998) 107.
[6] S. Hilaire, X. Wang, T. Luo, R.J. Gorte and J. Wagner, Appl. Catal. A 215 (2001) 271.
[7] X. Wang and R.J. Gorte, Appl. Catal. A 247 (2003) 157.
[8] X. Wang, R.J. Gorte and J.P. Wagner, J. Catal. 212 (2002) 225.
[9] R.W. Wunder and J. Phillips, J. Phys. Chem. 100 (1996) 14430.
[10] M. Tinkle and J.A. Dumesic, J. Catal. 103 (1987) 65.
[11] H. Okamoto, in *Phase Diagrams of Binary Iron Alloys*, H. Okamoto (ed.) (ASM International, Materials Park, OH, 1993) pp. 319–325 .
[12] J.W. Niemantsverdriet, J.A.C. van Kaam, C.F.J. Flipse and A.M. van der Kraan, J. Catal. 96 (1985) 58.
[13] Y.-H. Chin, R. Dagle, J. Hu, A.C. Dohnalkova and Y. Wang, Catal. Today 77 (2002) 79.